

Updating a simple model of lunar recession

R. Caimmi *

October 17, 2018

Abstract

A classical model of lunar recession is reviewed and updated, where input parameters are taken or inferred from earlier astronomical computation of insolation quantities on Earth back to 0.25 Gyr. Free parameters are (i) the transition age, $t_a - t^\ddagger$, where mean lunar recession velocity, \dot{a} , is suddenly lowered, and (ii) the merging age, $t_a - t^\ddagger$, where Earth-Moon distance (EMD), a , drops to zero, which relates to mean lunar recession velocity just after transition, \dot{a}^\ddagger . Predicted mean EMD and length of day (LOD) slightly overestimate their counterparts from the above mentioned astronomical computation. Predicted LOD, where the effect of atmospheric tides and nontidal processes is considered and supposed to be time independent, slightly underestimates a linear interpolation from paleontological data related to Phanerozoic, inferred in earlier investigations. If short-period ($\Delta t \approx 10^{-3}$ Gyr) EMD fluctuations ($\Delta a \approx \mp 0.5R_\oplus$), resulting from the above mentioned astronomical computation back to 0.25 Gyr, occur along the whole evolution of Earth-Moon system (EMS), then the predicted mean EMD is consistent with values inferred from three well studied paleontological data sets: Elatina-Reynella (ER), Big Cottonwood (BC), Weeli Wolli (WW), for $t_a - t^\ddagger = 0.25$ Gyr and $t_a - t^\ddagger = 6$ Gyr. The same holds for LOD where, in addition, computed values are consistent with a linear interpolation from paleontological data

**Physics and Astronomy Department, Padua University, Vicolo Osservatorio 3/2, I-35122 Padova, Italy. Affiliated up to September 30th 2014. Current status: Studioso Senior. Current position: in retirement due to age limits. email: roberto.caimmi@unipd.it fax: 39-049-8278212*

related to Proterozoic, inferred in earlier investigations. The situation is reversed if the effect of atmospheric tides and nontidal processes is taken into consideration and supposed to be time independent, in the sense that fitting curves relate to merging age in advance with respect to formation age. Accordingly, the above mentioned effect cannot be supposed as time independent during Proterozoic. In conclusion, the current model can be considered as a useful zeroth-order approximation to the evaluation of lunar recession and LOD. More accurate paleontological data, especially in connection with error evaluation, would be desirable in view of improved results and further constraints involving both Astronomy and Paleontology.

keywords - Earth-Moon system - tidal friction - lunar recession - length of day.

1 Introduction

The evolution of Earth-Moon system (EMS) has been debated for centuries since the beginning of the scientific revolution. Related references are mentioned in earlier investigations e.g., [2][16][25][9] and shall not be repeated here.

The driving mechanism lies in the lunar tidal friction, which acts along the following steps e.g., [25].

- (1) The gravitational force of the Moon raises a tidal bulge in the solid Earth and oceans.
- (2) Because of friction there is a delay in Earth's response, causing the tidal bulge to lead the Earth-Moon axis by a small angle.
- (3) The Moon exerts a torque on the tidal bulge that retards Earth's rotation, thereby increasing the length of day (LOD).
- (4) The torque that Earth's tidal bulge exerts on the Moon leads to an acceleration of the Moon's orbital motion, causing the Moon to recede from Earth.

While lunar recession is almost entirely due to tidal friction, LOD can be affected, in addition, by other processes such as core-mantle friction, atmospheric tides, mantle convection, macrodiffusion at the core-mantle boundary e.g., [10][8][3]. Tidal despinning is less or more effective according if continents are gathered to form a supercontinent, Pangaea say, or are spread over Earth surface, respectively e.g., [16][3].

Direct determination of lunar recession by laser ranging [5] yields a value that mildly changes back to 0.25 Gyr [9]. Extrapolation to earlier ages would imply catastrophic Earth-Moon close approach within 2 Gyr or less [8][26][25], which is in contradiction with inferred age of lunar rocks (brought back via Apollo missions) equal to about 4.5 Gyr e.g., [7][17][1]. Then the mean lunar recession before Phanerozoic (back to about 0.57 Gyr) had to be significantly lower than the current value and even the average value through Phanerozoic e.g., [26].

Paleotidal and paleorotational values can be inferred from fossil corals and molluscs e.g., [12][8][26][14][15][18][25]. More specifically, fine laminae are interpreted either as daily growth increments or as the record of the semidiurnal or diurnal tide, in accordance with the general growth habits of related current descendants. Modulation of the fine banding by the fortnightly or monthly tidal cycles and by the yearly seasonal cycle allows estimates of the number of days per year, the number of days per month, and the number of months per year [26].

In general, paleontological data are presented with no reliable error bands for both related age and inferred quantities which are quite large anyway e.g., [16]. An exception is concerned with at least three cases concerning precambrian cyclic rhythmites found on the following formations: (i) Weeli Wolli (WW), Western Australia, about 2.45 Gyr ago [26][20][21]; (ii) Big Cottonwood (BC), Utah, about 0.90 Gyr ago [14][15]; (iii) Elatina and Reynella Siltstone (ER), South Australia, about 0.62 Gyr ago [18][19][20][21][22][23][24]. For further details, an interested reader is addressed to the parent paper [25].

A nontrivial question is how to consider the above mentioned paleontological data with respect to the remaining ones. To this respect, an extreme case could be excluding the latter e.g., [25] and the opposite could be assigning equal statistical weight to all available data e.g., [3]. Comparison of model predictions to values inferred from observations would imply the former alternative, in that error bars are needed, while determination of empirical laws would prefer the latter alternative, where larger datasets are available.

Under restrictive but plausible assumptions, the mean Earth-Moon distance (EMD), a , in the past can be expressed in terms of the age, $t_a - t$ (t_a is the current EMS age), the current EMD, a_a , and the current mean lunar recession, $\langle \dot{a}_a \rangle$, which implies catastrophic Earth-Moon collision within 2 Gyr or less [8][26][25]. To avoid this discrepancy, a sudden reduction in mean lunar recession velocity at an assigned transition age is necessary [26][25]. Accordingly, model key parameters are the transition age, $t_a - t^\dagger$, and the merging age, $t_a - t^\ddagger$, where the latter has necessarily to take place in advance with respect to EMS formation age, $t_a - t_i$.

In this view, the merging age is an artefact of the model, in the sense

the Moon orbit becomes unstable when Roche limit or corotation limit is attained, and computation should be halted there. In addition, EMS birth has to be conceived as the earliest configuration where (quasi) equilibrium holds. To this respect, all proposed models of Moon formation e.g., [1] could be viable.

Though the above mentioned classical model of lunar recession has been used in the past e.g., [26][25], still detailed formulation and exploration of parameter space is lacking (to the knowledge of the author) and it could be a useful zeroth order approximation for more refined attempts. In addition, Moon formation is never explicitly mentioned (to the knowledge of the author) in dealing with paleotidal and paleorotational values which, on the other hand, could strengthen mutual connection between astronomical and paleontological data.

The current paper is aimed to review and update the classical model of lunar recession e.g., [26][25], according to the above considerations. The model and related input parameters are presented in Section 2 after a number of basic considerations. The results are shown in Section 3 and compared with their counterparts inferred from both astronomical computations (0-0.25 Gyr ago) [9] and paleontological data (0-2.5 Gyr ago) [26][16][25][3]. The discussion is performed in Section 4 and the conclusion makes the subject of Section 5.

2 A classical model of lunar recession

2.1 Boundary conditions

Let a two-body system be considered where the secondary, S (in particular, a satellite) undergoes circular orbits around the primary, P (in particular, a planet). Let the two bodies be rigid and spherical-symmetric. If a_1 and a_2 are radii of different orbits, the application of Kepler third law yields:

$$\left(\frac{P_1}{P_2}\right)^2 = \left(\frac{a_1}{a_2}\right)^3 ; \quad (1)$$

where P is the orbital period. In presence of satellite (secular) recession, the indexes, 1 and 2, can be related to different ages e.g., [4].

In the special case of negligible (with respect to unity) secondary-to-primary mass ratio, the lower limit of stable orbits, or Roche limit, is e.g., [6] Chap.VIII §212:

$$a_R = 2.4554 \left(\frac{\bar{\rho}_P}{\bar{\rho}_S}\right)^{1/3} R_P ; \quad \frac{M_S}{M_P} \ll 1 ; \quad (2)$$

where a_R is the orbital radius when the Roche limit is attained, $\bar{\rho}$ is the mean density, R the radius and M the mass. After performing little algebra, Eq. (2) translates into:

$$a_R = 2.4554 \left(\frac{M_P}{M_S} \right)^{1/3} R_S ; \quad \frac{M_S}{M_P} \ll 1 ; \quad (3)$$

in terms of masses instead of mean densities. The numerical coefficient on the right-hand side of Eqs. (2) and (3) can be approximated as $2^{4/3} \approx 2.5198$.

The orbital period of a stable ($a_S \geq a_R$) orbit is e.g., [1]:

$$P_S = 2\pi \left(\frac{a_S^3}{GM_P} \right)^{1/2} ; \quad M_S \ll M_P ; \quad (4)$$

where $G = 6.67408 \cdot 10^{-8} \text{ cm}^3/(\text{g s}^2)$ is the constant of gravitation. In the Roche limit ($a_S = a_R$) Eq. (4) reads:

$$P_R = 2\pi \left(\frac{a_R^3}{a_S^3 GM_P} \right)^{1/2} = \left(\frac{a_R}{a_S} \right)^{3/2} P_S ; \quad M_S \ll M_P ; \quad (5)$$

in agreement with Eq. (1).

With regard to EMS, $R_S = R_\odot = 1378 \text{ km}$, $M_S/M_P = M_\odot/M_\oplus = 0.0123 \ll 1$, and Eq. (3) reduces to:

$$a_R = 18487.1467 \text{ km} = 2.8985 R_\oplus ; \quad (6)$$

where R_\odot , M_\odot , $R_P = R_\oplus$, are Moon radius, Moon mass, Earth radius, respectively.

The particularization of Eq. (1) to the current EMS configuration, via Eq. (6) yields:

$$P_R = 6.9487 \text{ h} ; \quad (7)$$

where $a_\odot = 60.1426 R_\oplus$ and $P_\odot = 27.4404 \text{ d}$ have been inferred from an earlier investigation [9]. If EMS evolution is intended as a sequence of (quasi) equilibrium configurations, then lunar distance and orbital period are confined above a threshold of about $3R_\oplus$ and 7 h, respectively.

Turning to the general case, let T_P be the rotation period of the primary body. The corotation condition is $P_S = T_P$ e.g., [1] which, via Eq. (4), after little algebra reads:

$$a_C = \left(\frac{GM_P}{4\pi^2} \right)^{1/3} T_P^{2/3} ; \quad (8)$$

where $a_S = a_C$ is the orbital radius in presence of corotation. If the Roche limit coincides with the corotation limit, $a_R = a_C$, then $T_P = P_R$ via Eqs. (5) and (8). A secondary body orbitating below the corotation radius will spiral in towards the primary due to tides e.g., [1].

With regard to EMS, $M_P = M_\oplus = 5.9726 \cdot 10^{27}$ g and Eq. (8) reduces to:

$$a_C = 0.795989 R_\oplus \left(\frac{T}{h} \right)^{2/3} ; \quad (9)$$

where $T = T_\oplus$ is LOD at an assigned age.

For fluid masses in rigid rotation, a necessary condition for equilibrium (due to Poincaré) is e.g., [6] Chap. IX §240:

$$\Omega^2 < \Omega_P^2 = 2\pi G \bar{\rho}_P ; \quad (10)$$

where Ω is the angular velocity and the index, P, denotes Poincaré limit. Related Poincaré rotation period, $T_P = 2\pi/\Omega_P$, is inferred from Eq. (10) as:

$$T_P = \frac{2\pi}{(2\pi G \bar{\rho})^{1/2}} = 2\pi \left(\frac{2}{3} \frac{R^3}{GM} \right)^{1/2} ; \quad (11)$$

where the last equality holds for spherical bodies. Shorter periods, $T < T_P$, would imply fission or equatorial rings in centrifugal support e.g., [6] Chap. IX §§235-240. With regard to the Earth, $R = R_\oplus = 6378.1366 \cdot 10^5$ cm and Eq. (11) reduces to:

$$T_P = 1.149728 \text{ h} ; \quad (12)$$

which is a LOD lower limit for Earth stability.

In summary, sequences of EMS equilibrium configurations must necessarily satisfy the following boundary conditions:

$$a \geq a_R = 2.898518 R_\oplus ; \quad (13)$$

$$P \geq P_R = 6.948719 \text{ h} ; \quad (14)$$

radius and period of lunar orbit above Roche limit;

$$a \geq a_C = 0.795989 R_\oplus ; \quad (15)$$

radius of lunar orbit above corotation radius;

$$T \geq T_P = 1.149728 \text{ h} ; \quad (16)$$

LOD above Poincaré limit.

2.2 The model

According to the classical model of lunar recession e.g., [8][26][4][16][25][3], the following restrictions hold.

- (1) EMS evolution occurs along a sequence of (quasi) equilibrium configurations where the total angular momentum remains unchanged.
- (2) The driving mechanism is due to semidiurnal tidal friction on solid Earth + ocean, which causes angular momentum transfer from Earth spin to Moon revolution, increasing both LOD and lunar recession.
- (3) The tidal friction from the Sun is negligible with respect to the tidal friction from the Moon.
- (4) Earth and Moon mass distribution are spherical-symmetric in absence of tidal effects.
- (5) Earth and Moon mass and radius remain unchanged.
- (6) The Moon retains synchronous rotation.
- (7) Moon orbit retains circular and lying on the ecliptic plane.

For further details, an interested reader is addressed to the above quoted papers.

Within the framework of the classical model, EMD at the age, $t_a - t$, e.g., [26][25] and related recession velocity read:

$$\frac{a}{a_a} = \left[1 - \frac{13}{2}(t_a - t) \frac{\langle \dot{a}_a \rangle}{a_a} \right]^{2/13} ; \quad (17)$$

$$\frac{\dot{a}}{\langle \dot{a}_a \rangle} = \left[1 - \frac{13}{2}(t_a - t) \frac{\langle \dot{a}_a \rangle}{a_a} \right]^{-11/13} ; \quad (18)$$

and the inverse function is:

$$t_a - t = \frac{2}{13} \frac{a_a}{\langle \dot{a}_a \rangle} \left[1 - \left(\frac{a}{a_a} \right)^{13/2} \right] ; \quad (19)$$

where extrapolation to merging configuration, $a = 0$, yields:

$$t_a - t^\ddagger = \frac{2}{13} \frac{a_a}{\langle \dot{a}_a \rangle} ; \quad (20)$$

which marks the end of the sequence.

The substitution of Eq. (20) into (17) after little algebra yields:

$$\frac{a}{a_a} = \left[1 - \frac{t_a - t}{t_a - t^\ddagger} \right]^{2/13} = \left[\frac{(t_a - t^\ddagger) - (t_a - t)}{t_a - t^\ddagger} \right]^{2/13} ; \quad (21)$$

in terms of the merging age, $t_a - t^\ddagger$.

Merging configurations must be conceived as purely fictitious (unless EMS took birth from fission), keeping in mind sequences of (quasi) equilibrium configurations necessarily end by attaining the Roche limit. On the other hand, the merging age cannot occur in advance of EMS formation, as:

$$t_a - t_i \leq t_a - t^\ddagger ; \quad (22)$$

and sequences for which Eq. (22) is violated must be disregarded.

Using current values of EMD and mean lunar recession velocity, listed in Table 1, the merging age via Eq. (20) reads:

$$t_a - t^\ddagger = 1.516617 \text{ Gyr} ; \quad (23)$$

which is at odds with Eq. (22), keeping in mind $t_a - t_i \approx 4.5$ Gyr e.g., [1]. The above discrepancy could be avoided, provided mean lunar recession velocity was substantially reduced in the past with respect to the present e.g., [26][25].

More specifically, the simplest option is a single discontinuity at a transition age, $t_a - t^\dagger$, where $\dot{a}(t_a - t^\dagger)$ instantaneously drops to \dot{a}^\dagger . Accordingly, Eq. (17) is valid back to $t_a - t^\dagger$, as:

$$\frac{a^\dagger}{a_a} = \left[1 - \frac{13}{2}(t_a - t^\dagger) \frac{\langle \dot{a}_a \rangle}{a_a} \right]^{2/13} ; \quad (24)$$

in earlier ages, $t_a - t > t_a - t^\dagger$, Eqs. (17), (20), (21), translate into:

$$\frac{a}{a^\dagger} = \left[1 - \frac{13}{2}(t^\dagger - t) \frac{\langle \dot{a}^\dagger \rangle}{a^\dagger} \right]^{2/13} ; \quad (25)$$

$$t^\dagger - t^\ddagger = \frac{2}{13} \frac{a^\dagger}{\langle \dot{a}^\dagger \rangle} ; \quad (26)$$

$$\frac{a}{a^\dagger} = \left[1 - \frac{t^\dagger - t}{t^\dagger - t^\ddagger} \right]^{2/13} = \left[\frac{(t^\dagger - t^\ddagger) - (t^\dagger - t)}{t^\dagger - t^\ddagger} \right]^{2/13} ; \quad (27)$$

where $t^\dagger - t$ is the age since the transition age, $t_a - t^\dagger$. Accordingly, free parameters of the model are the transition age and the merging age.

Under the restrictive assumption LOD changes only via tidal friction, using angular momentum conservation and Kepler's third law yields [4]¹:

$$\left(\frac{a}{a_a}\right)^{1/2} + \frac{C_2}{13} \left(\frac{a}{a_a}\right)^{13/2} = -C_1 \frac{\Omega}{\Omega_a} + C_3 ; \quad (28)$$

$$C_1 = \frac{1}{4.93} ; C_2 = (0.46)^2 = 0.2116 ; C_3 = 1 + C_1 + \frac{C_2}{13} = 1.219117 ; (29)$$

where Ω is Earth angular velocity, C_1 is the current ratio of Earth spin angular momentum to Moon orbital angular momentum, C_2 is the current ratio of solar to lunar retarding torques acting on Earth, and C_3 is an integration constant e.g., [4].

In terms of LOD, $T = 2\pi/\Omega$, Eq. (28) after some algebra reads:

$$\frac{T}{T_a} = C_1 \left\{ C_3 - \left(\frac{a}{a_a}\right)^{1/2} \left[1 + \frac{C_2}{13} \left(\frac{a}{a_a}\right)^6 \right] \right\}^{-1} ; \quad (30)$$

and LOD variation rate after some algebra can be inferred from Eq. (30) as:

$$\frac{\dot{T}}{T_a} = \frac{1}{2} \frac{1}{C_1} \frac{T^2}{T_a^2} \left(\frac{a}{a_a}\right)^{-1/2} \frac{\dot{a}}{a_a} \left[1 + C_2 \left(\frac{a}{a_a}\right)^6 \right] ; \quad (31)$$

where the current value is:

$$\frac{\dot{T}_a}{T_a} = \frac{1}{2} \frac{1}{C_1} \frac{\dot{a}_a}{a_a} (1 + C_2) ; \quad (32)$$

finally, dividing each side of Eq. (31) by its counterpart of Eq. (32) yields:

$$\frac{\dot{T}}{T_a} \left(\frac{T}{T_a}\right)^{-2} = \frac{\dot{a}}{a_a} \left(\frac{a}{a_a}\right)^{-1/2} \frac{1 + C_2(a/a_a)^6}{1 + C_2} ; \quad (33)$$

where $\dot{a}_a = \langle \dot{a}_a \rangle$ for sake of brevity.

With regard to the transition age, $t_a - t^\dagger$, Eqs. (30) and (33) after some algebra translate into:

$$\frac{T}{T^\dagger} = C'_1 \left\{ C'_3 - \left(\frac{a}{a^\dagger}\right)^{1/2} \left[1 + \frac{C'_2}{13} \left(\frac{a}{a^\dagger}\right)^6 \right] \right\}^{-1} ; \quad (34)$$

$$\frac{\dot{T}}{T^\dagger} \left(\frac{T}{T^\dagger}\right)^{-2} = \frac{\dot{a}}{a^\dagger} \left(\frac{a}{a^\dagger}\right)^{-1/2} \frac{1 + C_2(a/a^\dagger)^6}{1 + C_2} ; \quad (35)$$

$$C'_1 = C_1 \frac{T_a}{T^\dagger} \left(\frac{a^\dagger}{a_a}\right)^{1/2} ; C'_2 = C_2 \left(\frac{a^\dagger}{a_a}\right)^6 ; C'_3 = C_3 \left(\frac{a^\dagger}{a_a}\right)^{-1/2} ; \quad (36)$$

¹The term, $(a_0/a)^6$ has to be replaced by $(a/a_0)^6$ in Eq. (2) therein, to be consistent with next Eq. (3).

Table 1: Values of input parameters used for computations, taken or inferred from an earlier investigation with regard to J2000.0 date [9]. The current lunar period is determined via Eq. (4). The difference with respect to current values is acceptably low except for \dot{T}_a .

parameter	value	caption
R_{\oplus}/km	6378.1366	equatorial Earth radius
R_{\odot}/km	1738	equatorial Moon radius
M_{\odot}/M_{\oplus}	0.0123000383	Moon-to-Earth mass ratio
T_a/h	23.934468	current length of day
$\dot{T}_a/(\text{ms}/\text{cy})$	2.675580	current change in length of day
a_a/R_{\oplus}	60.142611	current Earth-Moon distance
$\langle \dot{a}_a \rangle/(\text{cm}/\text{y})$	3.891229	current lunar recession velocity
P_{\odot}/d	27.440392	current lunar orbital period

where Eqs. (34) and (35) retain the formal expression of Eqs. (30) and (33), respectively, regardless of the transition age, provided related constants are redefined via Eq. (36).

In the special case of merging age, $a = 0$, Eq. (30) reduces to:

$$\frac{T^{\ddagger}}{T_a} = \frac{C_1}{C_3} = 0.1663826 \quad ; \quad (37)$$

accordingly, LOD (under the influence of tidal friction) attains a minimum value as:

$$T \geq T^{\ddagger} = 0.1663826 T_a = 3.982278 \text{ h} \quad ; \quad (38)$$

regardless of the sequence under consideration.

2.3 Input parameters

For dealing with a self-consistent set of input parameters, values are taken or inferred from an earlier investigation [9] as listed in Table 1. EMS evolution therein is considered within the framework of a new solution for astronomical computation of insolation quantities on Earth spanning from -0.25 Gyr to $+0.25$ Gyr. Related polynomial approximations for mean EMD and LOD read [9]:

$$\frac{a}{R_{\oplus}} = \sum_{k=0}^4 A_k \left(\frac{t_a - t}{\text{Gyr}} \right)^k \quad ; \quad (39a)$$

$$A_0 = \frac{a_a}{R_\oplus} = 60.142611 ; \quad A_1 = -6.100887 ; \quad A_2 = -2.709407 ; \quad (39b)$$

$$A_3 = -1.366779 ; \quad A_4 = -1.484062 ; \quad (39c)$$

$$\frac{T}{h} = \sum_{k=0}^4 B_k \left(\frac{t_a - t}{\text{Gyr}} \right)^k ; \quad (40a)$$

$$B_0 = \frac{T_a}{h} = 23.934468 ; \quad B_1 = -7.432167 ; \quad B_2 = -0.727046 ; \quad (40b)$$

$$B_3 = -0.409572 ; \quad B_4 = -0.589692 ; \quad (40c)$$

where a appears in place of $\langle a \rangle$ for sake of brevity and the terms related to $k > 4$ are negligible in both cases.

In particular, current mean lunar velocity recession and LOD variation rate are inferred from Eqs. (39) and (40), respectively, as listed in Table 1. While the former result is consistent with the current mean lunar velocity recession inferred from lunar laser ranging, $\langle \dot{a}_a \rangle = (3.82 \mp 0.07) \text{ cm/y}$ [5], the latter substantially exceeds LOD variation rates mentioned in different investigations e.g., $\dot{T}_a = (2.3 \mp 0.1) \text{ ms/cy}$ [16][3]; $\dot{T}_a = (2.50 \mp 0.01) \text{ ms/cy}$ [11].

A comparison between numerical integration and analytical approximation discloses the occurrence of short-period ($\Delta t \approx 10^{-3} \text{ Gyr}$) EMD fluctuations ($\Delta a/R_\oplus \approx \mp 0.5$) around the local mean value [9]. Accordingly, EMD evolution lies within a band, centered on the local mean value, where the vertical width equals about one Earth radius. A choice of input parameters as listed in Table 1 leaves two free parameters, namely the transition age, $t_a - t^\dagger$, and the merging age, $t_a - t^\ddagger$.

Computer runs were performed for the following cases: (a) $(t_a - t^\dagger)/\text{Gyr} = 0.57$; $(t_a - t^\ddagger)/\text{Gyr} = 1.516617$ (no discontinuity in $\langle \dot{a} \rangle$), 2.0, 2.5, ..., 4.5, and (b) $(t_a - t^\dagger)/\text{Gyr} = 0.25$; $(t_a - t^\ddagger)/\text{Gyr} = 1.516617$ (no discontinuity in $\langle \dot{a} \rangle$), 2.0, 2.5, ..., 4.5, 5.0, 6.0, 7.0, 10.0. More specifically, a discontinuity in lunar recession velocity takes place (more or less) at the transition between Proterozoic and Phanerozoic in the former alternative, and at formation and deformation of Pangaea supercontinent in the latter alternative e.g., [16][3].

3 Results

With regard to the past 0.25 Gyr, $0 \leq (t_a - t)/\text{Gyr} \leq 0.25$, predicted mean EMD (in Earth radii), a/R_\oplus , vs age, $t_a - t$, according to Eq. (17), is shown in Fig. 1 as a dashed line e.g., [26][25]. By comparison, mean EMD inferred

from astronomical computation within the framework of a new solution for the insolation quantities on Earth, according to Eq. (39), is shown in Fig. 1 as a full line inside a band [9]. The band vertical width ($\Delta a/R_{\oplus} \approx 1$) is owing to short-period ($\Delta t \approx 10^{-3}$ Gyr) EMD fluctuations [9]. An inspection of Fig. 1 discloses Eq. (17) is in close agreement with its counterpart, Eq. (39), related to a more sophisticated model [9].

Dotted straight lines define a special point, (0.192150014, 58.85857007), on the central full curve, for which the ratio of mean EMD to lunar diameter reads $a/(2R_{\oplus}) = 108$. The occurrence of short-period fluctuations implies the above value can be attained within a range, $0.12 \lesssim (t_a - t)/\text{Gyr} \lesssim 0.25$.

Predicted LOD due to tidal friction, T/h , vs age, $(t_a - t)/\text{Gyr}$, according to Eq. (30), is shown in Fig. 2 as a dashed line. By comparison, LOD inferred from astronomical computation within the framework of a new solution for the insolation quantities on Earth, according to Eq. (40), is shown in Fig. 2 as a full line [9]. An inspection of Fig. 2 discloses Eq. (30) is in close agreement with its counterpart, Eq. (40), related to a more sophisticated model [9].

Dotted straight lines define a special point, (0.192150014, 22.47646196), on the full curve, for which the ratio of mean EMD to lunar diameter reads $a/(2R_{\oplus}) = 108$.

The dot-dashed line is a linear interpolation from paleontological data, $T/h = T_a/h - 4.98(t_a - t)/\text{Gyr}$, shown in earlier investigations [16][3]. A non-linear trend also inferred from paleontological data [16][3] is shown as squares.

Concerning whole EMS evolution, assumed to start from $(t_a - t_i)/\text{Gyr} = 4.57$, and a transition age, $(t_a - t^\dagger)/\text{Gyr} = 0.57$, predicted EMD (in Earth radii), a/R_{\oplus} , vs age, $(t_a - t)/\text{Gyr}$, is shown in Fig. 3 as full lines for selected merging ages, $(t_a - t^\ddagger)$, or selected mean lunar recession velocities just after the transition age, $\langle \dot{a}^\dagger \rangle$, via Eq. (20), as listed in Table 2. All features appearing in Fig. 1 are included within $0 \leq (t_a - t)/\text{Gyr} \leq 0.25$, but dotted straight lines define a special point, (0.198499271, 58.85857007), on the dashed curve therein, for which the ratio of mean lunar distance to lunar diameter reads $a/(2R_{\oplus}) = 108$. Dashed vertical straight lines mark the selected transition age, $(t_a - t^\dagger)/\text{Gyr} = 0.57$ (left) and the assumed EMS age, $(t_a - t_i)/\text{Gyr} = 4.57$ (right). The Roche limit, $a_R/R_{\oplus} = 2.898518$, is defined by a horizontal straight line. Values inferred from paleontological data from earlier investigations [25] are plotted as diamonds, related to different authors when appropriate [25]. Source of data (from the left to the right) are: ER, BC (lower value preferred), WW (upper value preferred) [25].

Predicted LOD due to tidal friction, T/h , vs age, $(t_a - t)/\text{Gyr}$, according to Eq. (30), is shown in Fig. 4 as full lines for a transition age, $(t_a - t^\dagger)/\text{Gyr} = 0.57$, and selected merging ages, $(t_a - t^\ddagger)$, or selected mean lunar recession

Table 2: Mean lunar velocity recession just after the transition age, $\langle \dot{a}^\dagger \rangle$, for different selected merging ages, $t_a - t^\ddagger$, with regard to transition ages, $t_a - t^\ddagger = 0.57$ Gyr (left column) and 0.25 Gyr (right column). The first row relates to absence of discontinuity at the transition age in connection with a merging age, $t_a - t^\ddagger = 1.516617$ Gyr. Accordingly, $\langle \dot{a} \rangle = 5.7982$ cm/y (left column) and 4.5319 cm/y (right column) just before transition, regardless of the merging age. All cases are plotted in Figs.3-4 (left column) and 5-6 (right column).

$\frac{t_a - t^\ddagger}{\text{Gyr}}$	$\langle \dot{a}^\dagger \rangle$ cm/y	
1.5	5.7982	4.5319
2.0	3.8383	3.2801
2.5	2.8439	2.5512
3.0	2.2587	2.0873
3.5	1.8733	1.7662
4.0	1.6002	1.5307
4.5	1.3966	1.3506
5.0		1.2085
6.0		0.99830
7.0		0.85041
10.0		0.58874
$+\infty$	0	0

velocities just after the transition age, $\langle \dot{a}^\dagger \rangle$, via Eq. (20), as listed in Table 2. All features appearing in Fig. 2 are included within $0 \leq (t_a - t)/\text{Gyr} \leq 0.25$, but dotted straight lines define a special point, (0.198499271, 22.50719109), on the dashed curve therein, for which the ratio of mean lunar distance to lunar diameter reads $a/(2R_\odot) = 108$.

Dashed vertical straight lines mark the selected transition age, $(t_a - t^\dagger)/\text{Gyr} = 0.57$ (left) and the assumed EMS age, $(t_a - t_i)/\text{Gyr} = 4.57$ (right). Symbol captions are as in Fig. 2 (squares) and Fig. 3 (diamonds). Dashed horizontal straight lines mark the Roche limit, $T_R/h = 6.948719$, the merging limit, $T^\ddagger/h = 3.982278$, and the Earth Poincaré limit, $T_P/h = 1.149728$.

Dot-dashed lines are linear interpolations from paleontological data, $T/h = 23.934468 - 4.98(t_a - t)/\text{Gyr}$, $0 \leq (t_a - t)/\text{Gyr} \leq 0.64$, and $T/h = 21.368068 - 0.97(t_a - t)/\text{Gyr}$, $0.64 \leq (t_a - t)/\text{Gyr} \leq 2.50$ [16][3], extended back to $(t_a - t_i)/\text{Gyr} = 4.57$.

An inspection of Figs. 3 and 4 discloses the most accurately inferred ER value [25] cannot be fitted to model curves even in the extreme case of no lunar recession after transition age (full horizontal straight line). Clearly the situation is reversed if the transition age is closer to the present. Then a later transition age, arbitrarily chosen as $t_a - t^\dagger = 0.25$ Gyr, has to be considered. The results are plotted in Figs. 5 and 6, where captions are the same as in Figs. 3 and 4, respectively.

Curves related to very early merging ages, $5 \lesssim (t_a - t^\dagger)/\text{Gyr} \lesssim 10$, are found to be consistent with ER and preferred WW value. The related range of mean lunar recession velocity just after the transition age, via Table 2 reads $1.21 \gtrsim \langle \dot{a}^\dagger \rangle /(\text{cm/y}) \gtrsim 0.60$, about 3-6 times lower than the current value.

Curves within a narrower range, $5 \lesssim (t_a - t^\dagger)/\text{Gyr} \lesssim 7$, are found to be consistent with both ER, preferred WW and unpreferred BC value [25], or $1.2 \gtrsim \langle \dot{a}^\dagger \rangle /(\text{cm/y}) \gtrsim 0.89$ via Table 2, where $\langle \dot{a}^\dagger \rangle /(\text{cm/y}) \approx 4.5$ just before transition.

Further restriction arises in dealing with LOD, Fig. 6, where $5 \lesssim (t_a - t^\dagger)/\text{Gyr} \lesssim 6$ is found following a similar procedure, or $1.2 \gtrsim \langle \dot{a}^\dagger \rangle /(\text{cm/y}) \gtrsim 0.99$, which could be shifted downwards if processes different from solid Earth + ocean tidal friction are effective in lowering LOD.

4 Discussion

Results from models of lunar recession need some caution, in the sense related computer runs start at present and go back into the past. A necessary restrictive assumption is that minor mergers and close encounters due to large-mass

asteroids had negligible effects on EMS evolution. Models implying merging ages in advance with respect to formation age, $t_a - t^\ddagger < t_a - t_i \approx 4.5$ Gyr, must be disregarded, which is the case of continuous mean lunar recession velocity, as shown in Figs. 3 and 5. Accordingly, key input parameters are the merging age and the transition age, $t_a - t^\ddagger$, where mean lunar recession velocity is suddenly reduced.

Remaining input parameters are taken or inferred from a solution for astronomical computation of insolation quantities on Earth within the range, $-0.25 \leq (t_a - t)/\text{Gyr} \leq +0.25$ [9], to which the prediction of the current model [26][25] satisfactorily fit, as shown in Figs. 1 and 2. In particular, input current mean lunar recession velocity and LOD variation read $\langle \dot{a}_a \rangle = 3.89$ cm/y and $\dot{T}_a = 2.68$ ms/cy, respectively [9], against $\langle \dot{a}_a \rangle = (3.82 \mp 0.07)$ cm/y inferred from lunar laser ranging experiment [5] and $\dot{T}_a = (2.50 \mp 0.01)$ ms/cy determined from solid Earth + ocean tidal friction [11].

Predicting LOD implies further problems, as lunar recession occurs only via tidal friction while LOD depends, in addition, on atmospheric tides and nontidal processes e.g., [16][9][3]. The current model works in presence of tidal friction only, which implies a LOD lower limit, keeping in mind the above mentioned additional effects act in the opposite direction i.e. increasing Earth spin. On the other hand, the model can be extended to the special case where the contribution from atmospheric tides and nontidal processes is time independent i.e. related LOD variation maintains the current value, $\Delta \dot{T}_a = (-0.10 - 0.55)$ ms/cy = -0.65 ms/cy [11].

A comparison between model predictions and paleontological data inferred from fossil corals and molluscs e.g., [12][8][26][14][15][18][25] can be made in a twofold manner, according if lunar recession or LOD are involved.

With regard to lunar recession, empirical values are inferred from the following formations: WW [26][20][21], BC [14][15], ER [18][19][20][21][22][23][24], where a collection appears in a later investigation [25]. For a transition age fixed at the late Precambrian, $t_a - t^\ddagger = 0.57$ Gyr, even if no lunar recession occurs at earlier ages, predicted EMD cannot fit to ER and WW data, while cases where the merging age is not in advance with respect to the formation age, $t_a - t^\ddagger \geq t_a - t_i \approx 4.5$ Gyr, are marginally consistent with BC data, as shown in Fig. 3.

Conversely, a transition age selected on the late Permian, $t_a - t^\ddagger = 0.25$ Gyr, yields acceptable cases, $5 \leq (t_a - t^\ddagger)/\text{Gyr} \leq 7$, where predicted EMD fits to ER, BC (unpreferred value) and WW (preferred value) data, as shown in Fig. 5. In addition, acceptable cases cannot fit to BC (preferred value) data, which implies at least one model assumption has to be released, provided data under discussion are correct, namely mean lunar recession velocity underwent several (instead of a single) discontinuities in the past.

The above mentioned discrepancy could be lowered by the occurrence of short-period ($\Delta t \approx 10^{-3}$ Gyr) EMD fluctuations ($\mp \Delta a \approx 0.5R_{\oplus}$), which were established back to 0.25 Gyr via astronomical computations [9]. If fluctuations of the kind considered took place back to 2.50 Gyr, it cannot be excluded EMD inferred from ER and WW data relate to a fluctuation maximum i.e. in excess of about $0.5R_{\oplus}$ with respect to related mean EMD, and EMD inferred from BC data relate to a fluctuation minimum i.e. in defect of about $0.5R_{\oplus}$ with respect to related mean EMD. Accordingly, the preferred EMD inferred from BC data [25] should be incremented by about $1R_{\oplus}$, passing from $(54.7 \mp 0.7)R_{\oplus}$ to $(55.7 \mp 0.7)R_{\oplus}$, which could be consistent with the unpreferred EMD inferred from BC data, equal to $57.1R_{\oplus}$ where the error is not reported [25].

Earlier applications of the current model yield similar results e.g., [26][25], regardless of (slightly different) values of input parameters. The current choice, listed in Table 1, makes a set of homogeneous data from a single source [9], which ensures consistency with astronomical computations, as shown in Figs. 1 and 2.

With regard to LOD, in addition to ER, BC, and WW data, different linear interpolations are available for Proterozoic and Phanerozoic e.g., [16][3], as:

$$T = T_a - 4.98(t_a - t) ; \quad 0 \leq t_a - t \leq t_a - t^* ; \quad (41a)$$

$$T = T'_a - 0.97(t_a - t) ; \quad t_a - t^* \leq t_a - t \leq t_a - t_i \quad (41b)$$

where $T_a = 23.934468$ h is the current (2000.0 JC date) LOD [9], T is the LOD at the age, $t_a - t$, and $t_a - t^* = 0.64$ Gyr.

The intercept, T'_a , can be determined keeping in mind Eqs. (41a) and (41b) both hold at the intersection point of related straight lines. The result is:

$$T'_a = T_a - (4.98 - 0.97)(t_a - t^*) = 21.368068 \text{ h} ; \quad (42)$$

and, in addition, $T^* = T_a - 4.98(t_a - t^*) = 20.747268$ h via Eq. (41).

Predicted LOD agrees to an acceptable extent with its counterpart inferred from astronomical computations [9], with a maximum discrepancy of 12 m at $t_a - t = 0.25$ Gyr. The contrary holds with respect to inferred (from paleontological data) LOD, Eq. (41a), where the maximum discrepancy amounts to 30 m at the same age, which is worsened considering a nonlinear trend, as shown in Fig. 2.

This is why predicted LOD is affected only by tidal friction in models under discussion [26][25][9], while inferred (from paleontological data) LOD

also includes atmospheric tides and nontidal processes such as mantle convection and iron macrodiffusion, which act in opposite sense with respect to tidal friction e.g., [16][9][11][3].

More specifically, the contribution from total solid Earth + ocean to current LOD variation is evaluated as (2.50 ∓ 0.01) ms/cy, and the contribution from atmospheric tides and nontidal processes as (-0.10 ∓ 0.01) ms/cy and (-0.55 ∓ 0.01) ms/cy, respectively [11]. Then the global contribution to current LOD variation amounts to (1.85 ∓ 0.01) ms/cy. Accordingly, the input current LOD variation, $\dot{T}_a = 2.68$ ms/cy, relates to the contribution from total solid Earth + ocean, while empirical LOD variation inferred from linear interpolation, $\dot{T}_a = 4.98$ h/Gyr ≈ 1.79 ms/cy, relates to the global contribution.

Under the restrictive assumption of time independent contribution from atmospheric tides and nontidal processes, $\Delta T/(t_a - t) = \text{const}$, using the above mentioned values yields $\Delta T/(t_a - t) = 0.65$ ms/cy, or:

$$\frac{\Delta T}{\text{h}} = \frac{65}{36} \frac{t_a - t}{\text{Gyr}} ; \quad (43)$$

where $T + \Delta T$ is the LOD at the age, $t_a - t$, due to total solid Earth + ocean tidal friction (T) with the addition of atmospheric tides and nontidal processes (ΔT). Related explicit form via Eqs. (30) and (43) reads:

$$\frac{T + \Delta T}{T_a} = C_1 \left\{ C_3 - \left(\frac{a}{a_a} \right)^{1/2} \left[1 + \frac{C_2}{13} \left(\frac{a}{a_a} \right)^6 \right] \right\}^{-1} + \frac{65}{36} \frac{t_a - t}{T_a} \frac{\text{h}}{\text{Gyr}} ; \quad (44)$$

which, in the special case of merging age, $a = 0$, $T = T^\ddagger$, reduces to:

$$T^\ddagger + \Delta T^\ddagger = \frac{C_1}{C_3} T_a + \frac{65}{36} (t_a - t^\ddagger) = 3.982659 \text{ h} + \frac{65}{36} (t_a - t^\ddagger) \frac{\text{h}}{\text{Gyr}} ; \quad (45)$$

that is a straight line in the variables, T^\ddagger and $t_a - t^\ddagger$.

Turning to the general case, the curve described by Eq. (44) is plotted in Fig. 2 as a dotted line, which is satisfactorily close to the interpolation line (dot-dashed) inferred from paleontological data, Eq. (41a). Fitting to an inferred nonlinear trend [16][3], plotted in Fig. 2 as squares, would need several (instead of a single) discontinuities in LOD variation, taking due account of, say, Pangaea formation and deformation e.g., [16][3].

An extension of inferred (from paleontological data) interpolation line to Archean and, fictiously, to EMS formation age, could be illustrative for comparison with predicted LOD, as shown in Figs. 4 and 6. To this aim, a choice must be done of what is the better empirical evidence among ER,

BC, WW data [25] on one hand, and inferred linear trend considering the above mentioned data as representative as the remaining ones [3] on the other hand. In fact, inferred linear interpolation lies below ER value and more or less in the middle of preferred and unpreferred BC and WW values. Both alternatives shall be considered in the following.

If the better empirical evidence of LOD relates to ER, BC and WW data, current models yield acceptable fits with regard to (i) late transition ages, and (ii) unpreferred BC value, as shown in Fig. 6 for curves related to merging ages, $5 \leq (t_a - t^\ddagger)/\text{Gyr} \leq 6$.

If the better empirical evidence of LOD relates to inferred linear interpolations, current models provide acceptable fits for late transition ages, as shown in Fig. 6 for curves related to merging ages, $(t_a - t^\ddagger)/\text{Gyr} \approx 6$.

In addition, errors on age of ER, BC and WW formation are not available e.g., [25] and for this reason an uncertainty of ∓ 0.05 Gyr has arbitrarily been assumed in plotting related values, even if larger uncertainties are probably expected.

Keeping into due account the (time independent) effect of atmospheric tides and nontidal processes, the situation is worsened as shown in Figs. 7 and 8, in the sense the merging age would be in advance with respect to the formation age. To avoid this inconsistency, the above mentioned effect should increase going back in time.

In conclusion, predicted LOD satisfactorily fits to both ER, BC, WW data and inferred linear interpolations with regard to late transition ages, $t_a - t^\ddagger \approx 0.25$ Gyr, and merging ages, $t_a - t^\ddagger \approx 6$ Gyr, leaving aside the effect of atmospheric tides and nontidal processes. Suitable choices of the above mentioned input parameters could better reproduce empirical values, but the main result is current models are consistent with the data in spite of restrictive assumptions.

On the other hand, a linear LOD-age relation is a zeroth-order approximation, as shown in Figs. 2, 4, 6, 7, 8, by comparison with data from earlier investigations [16][3], plotted as squares. A nonlinear trend could be owing to e.g., occurrence and persistence of a supercontinent associated to a deep superocean [16][3]. Even in this context, the current model could fit to the data if several (instead of a single) transition ages are considered, where mean lunar recession velocity suddenly drops to a lower value. To this aim, the effect (impacts or close encounters) of large-mass asteroids should be analysed in detail.

5 Conclusion

The evolution of Earth-Moon system (EMS) relates to several different disciplines, such as Astronomy, Geodesy, Geophysics, Oceanology, Geology, Paleontology, where comparison between theoretical predictions and results from data collections could imply constraints within all the involved fields. In this view, a classical model [26][4][25] has been reviewed and updated to many extents.

First, a homogeneous set of input parameters has been taken from earlier astronomical computations on insolation quantities on Earth spanning from -0.25 Gyr to $+0.25$ Gyr [9].

Second, predicted Earth-Moon distance (EMD) for assigned transition age, $t_a - t^\dagger$, and merging age, $t_a - t^\ddagger$, has been considered keeping in mind acceptable cases necessarily imply merging age in advance with respect to formation age, $t_a - t_i$.

Third, the presence of short-period ($\Delta t \approx 10^{-3}$ Gyr) EMD fluctuations ($\Delta a \approx \mp 0.5R_\oplus$) from astronomical computations [9], if typical of the whole evolution, implies uncertainty bands around $a(t)$ curves of thickness about $\mp 0.5R_\oplus$ and values inferred from paleontological data affected by an additional error, $\Delta a \approx \mp 0.5R_\oplus$, if related to mean (over a typical fluctuation period) EMD.

The main results of the present paper can be summarized as follows.

- (1) Predicted EMD and length of day (LOD) slightly overestimate their counterparts from astronomical computation of insolation quantities on Earth back to 0.25 Gyr [9].
- (2) Predicted LOD, when a time independent effect via atmospheric tides and nontidal processes is considered [11], slightly underestimates a linear interpolation from paleontological data related to Phanerozoic era [16][3].
- (3) For assigned transition age and merging age, predicted EMD and LOD cannot fit to their counterparts inferred from ER, BC and WW data, unless unpreferred instead of preferred values [25] are considered for BC data. Related difference in EMD appears comparable to amplitude in short-period fluctuations from astronomical computations during the late Phanerozoic [9]. Accordingly, a transition age, $t_a - t^\dagger = 0.25$ Gyr and a merging age, $t_a - t^\ddagger = 6$ Gyr, yield an acceptable fit. The situation is reversed if a time independent effect via atmospheric tides and nontidal processes is considered, in the sense that fitting curves relate to merging age in advance with respect to formation age.

- (4) For assigned transition age, $t_a - t^\dagger = 0.25$ Gyr and merging age, $t_a - t^\ddagger = 6$ Gyr, predicted LOD is consistent with inferred linear interpolation to paleontological data [16][3]. The situation is reversed if a time independent effect via atmospheric tides and nontidal processes is considered, in the sense that fitting curves relate to merging age in advance with respect to formation age.

Even if LOD variation was not linear in time e.g., [16][3], the current model remains valid as a zero-th order approximation. Further refinement would be desirable in dealing with paleontological data, in connection with error evaluation.

Acknowledgements

Thanks are due to S. Lambert for fruitful e-mail correspondance.

References

- [1] E. Asphaug, Impact Origin of the Moon?, *Annual Review of Earth and Planet Sciences* 42 (2014), 551-578.
- [2] P. Brosche, Tidal friction in the Earth-Moon system, *Philosophical transactions of the Royal Society of London, Ser. A* 313 (1984), 71-75.
- [3] C. Denis, K.R. Rybicki, A.A. Schreider, S. Tomecka-Suchoń, P. Varga, Length of the day and evolution of the Earth's core in the geological past, *Astronomische Nachrichten* 332 (2011), 24-35.
- [4] F.-L. Deubner, Discussion on Late Precambrian tidal rhythmites in South Australia and the history of the Earth's rotation, *Journal of the Geological Society of London* 147 (1990), 1083-1084.
- [5] J.O. Dickey, P.L. Bender, J.E. Faller, X.X. Newhall, R.L. Ricklefs, J.G. Ries, P.J. Shelus, C. Veillet, A.L. Whipple, J.R. Wiant, et al, Lunar Laser Ranging: A Continuing Legacy of the Apollo Program, *Science* 265 (1994), 482-490.
- [6] J. Jeans, *Astronomy and Cosmogony* (1929), Dover Publications, New York, 1961.
- [7] Z. Kopal, *The Moon in the Post-Apollo Era*, D. Reidel Publishing Company, Dordrecht, 1974.

- [8] K. Lambeck, *The Earth's Variable Rotation*, Cambridge University Press, New York, 1980.
- [9] J. Laskar, P. Robutel, F. Joutel, M. Gastineau, A.C.M. Correia, B. Levrard, A long-term numerical solution for the insolation quantities of the Earth, *Astronomy and Astrophysics* 428 (2004), 261-285.
- [10] E. Majewski, *Thermodynamic Model of the Core-mantle Boundary*, Publications of the Institute of Geophysics, Polish Academy of Sciences A 25 (1995), 1-59.
- [11] P.M. Mathews, S.B. Lambert, Effect of mantle and ocean tides on the Earth's rotation rate, *Astronomy and Astrophysics* 493 (2009), 325-330.
- [12] C.T. Scrutton, Periodic growth features in fossil organisms and the length of the day and month, in *Tidal Friction and the Earth's Rotation*, edited by P. Brosche and J. Sündermann, pp. 154-196, Springer-Verlag, New York, 1978.
- [13] C.P. Sonett, E.P. Kvale, A. Zakharian, M.A. Chan, T.M. Demko, Late Proterozoic and Palaeozoic tides, retreat of the Moon, and rotation of the Earth, *Science* 273 (1996), 100-104.
- [14] C.P. Sonett, A. Zakharian, E.P. Kvale, Ancient tides and length of day: Correction, *Science* 274 (1996), 1068-1069.
- [15] C.P. Sonett, M.A. Chan, Neoproterozoic Earth-Moon dynamics: Rework of the 900 Ma Big Cottonwood Canyon tidal rhythmites, *Geophysical Research Letters* 25 (1998), 539-542.
- [16] P. Varga, C. Denis, T. Varga, Tidal Friction and its Consequences in Palaeogeodesy, in the *Gravity Field Variations and in Tectonics*, *Journal of Geodynamics* 25 (1998), 61-84.
- [17] P. Varga, K.R. Rybicki, C. Denis, Comment on the paper "Fast tidal cycling and the origin of life" by Richard Lathe, *Icarus*, 180 (2006), 274-276.
- [18] G.E. Williams, Late Precambrian tidal rhythmites in South Australia and the history of the Earth's rotation, *Journal of the Geological Society of London* 146 (1989), 97-111.
- [19] G.E. Williams, Precambrian tidal sedimentary cycles and Earth's paleorotation, *Eos Transactions AGU* 70 (1989), 33 and 40-41.

- [20] G.E. Williams, Tidal rhythmites: Geochronometers for the ancient Earth-Moon system, *Episodes* 12 (1989), 162-171.
- [21] G.E. Williams, Key to the history of the Earth's rotation and the lunar orbit, *Journal of Physics of Earth* 38 (1990), 475-491.
- [22] G.E. Williams, Upper Proterozoic tidal rhythmites, South Australia: Sedimentary features, deposition, and implications for the earth's paleorotation, in *Clastic Tidal Sedimentology*, edited by D. G. Smith G.E. Reinson, B.A. Zaitlan, R.A. Rahmani, Canadian Society of Petroleum Geologists Memoir 16 (1991), 161-177.
- [23] G.E. Williams, History of Earth's rotation and the Moon's orbit: A key datum from Precambrian tidal strata in Australia, *Australian Journal of Astronomy*, 5 (1994), 135-147.
- [24] G.E. Williams, Precambrian length of day and the validity of tidal rhythmite paleotidal values, *Geophysical Research Letters*, 24 (1997), 421-424.
- [25] G.E. Williams, Geological Constraints on the Precambrian History of Earth's Rotation and the Moon's Orbit, *Reviews of Geophysics* 38 (2000), 37-59.
- [26] J.C.G. Walker, K.J. Zahnle, Lunar nodal tide and distance to the moon during the Precambrian, *Nature* 320 (1986), 600-602.

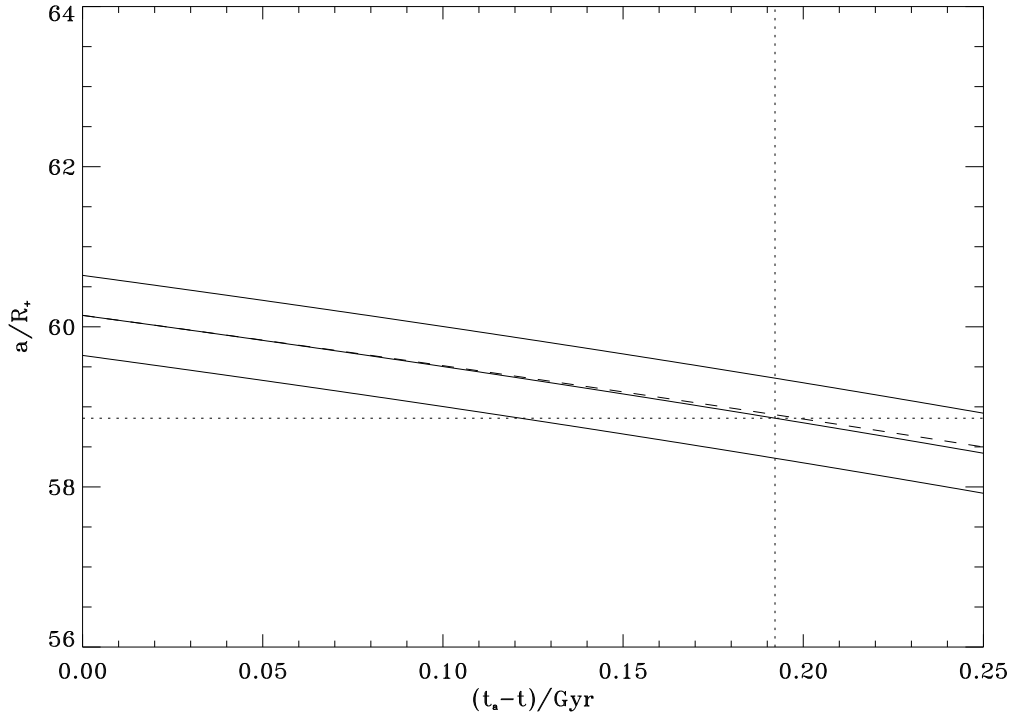


Figure 1: Predicted mean lunar distance (EMD, in Earth radii), a/R_{\oplus} , vs age (Gyr, back in time since J2000.0 date), $t_a - t$, for past 0.25 Gyr, according to Eq. (17), dashed line, and Eq. (39), full line within the band. The band vertical width ($\Delta a/R_{\oplus} \approx 1$) is owing to short-period ($\Delta t \approx 10^{-3}$ Gyr) EMD fluctuations. Dotted straight lines define a special point, (0.192150014, 58.85857007), on the central full curve for which the ratio of mean lunar distance to lunar diameter reads $a/(2R_{\odot}) = 108$. See text for further details.

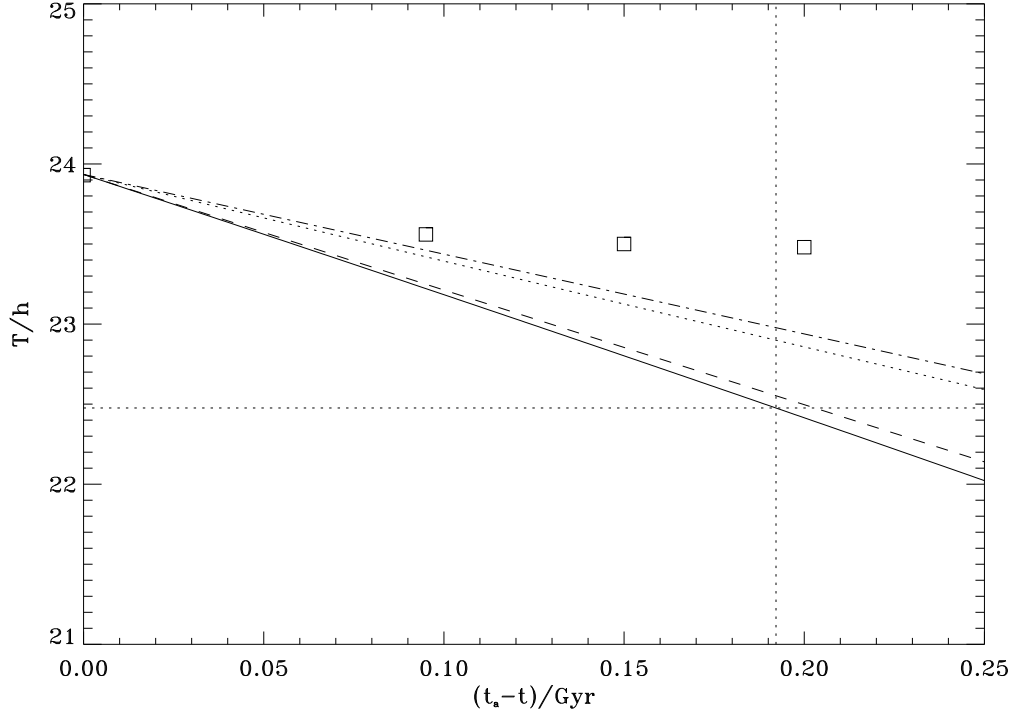


Figure 2: Predicted length of day (LOD) due to tidal friction, T/h , vs age (Gyr, back in time since J2000.0 date), $t_a - t$, for past 0.25 Gyr, according to Eq. (30), dashed line, and Eq. (40), full line. Dotted straight lines define a special point, $(0.192150014, 22.47646196)$, on the full curve for which the ratio of mean lunar distance to lunar diameter reads $a/(2R_{\odot}) = 108$. A linear interpolation from paleontological data is plotted as a dot-dashed line. A nonlinear trend also inferred from paleontological data is shown as squares. Predicted LOD including time independent effects from atmospheric tides and nontidal processes is represented as a dotted curve. See text for further details.

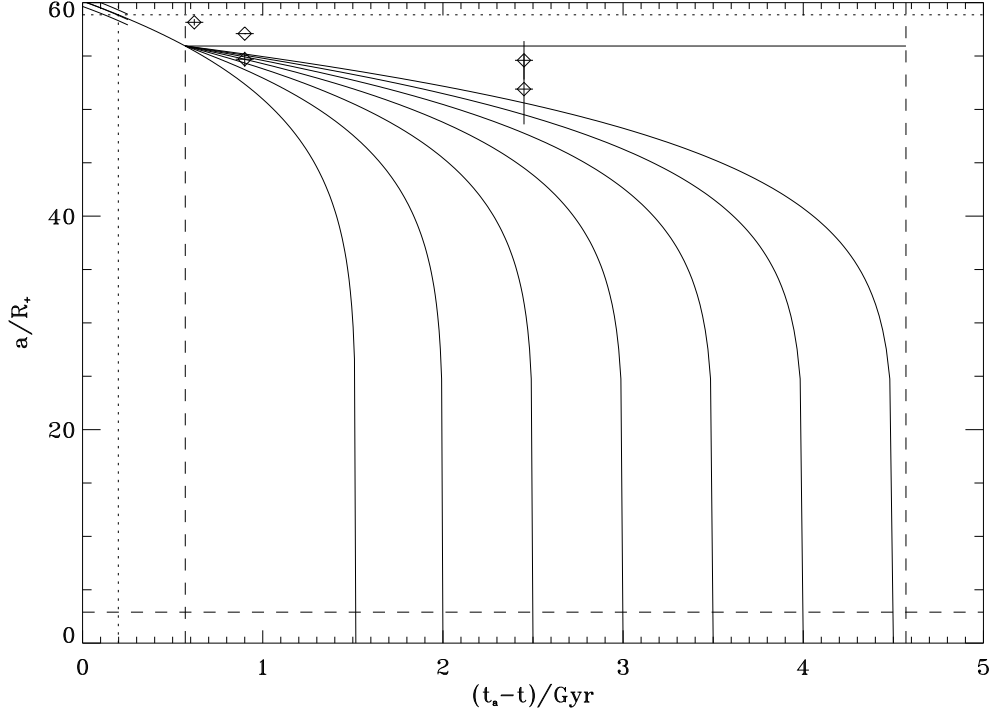


Figure 3: Predicted mean lunar distance (EMD, in Earth radii), a/R_{\oplus} , vs age (Gyr, back in time since J2000.0 date), $t_a - t$, for past 4.57 Gyr, according to Eq. (17), for different merging ages (from the left to the right), $(t_a - t^{\dagger})/\text{Gyr} = 1.516617, 2.0, 2.5, 3.0, 3.5, 4.0, 4.5, +\infty$ (no lunar recession). All features appearing in Fig. 1 are included within $0 \leq (t_a - t)/\text{Gyr} \leq 0.25$, but dotted straight lines define a special point, $(0.198499271, 58.85857007)$, on the dashed curve therein, for which the ratio of mean lunar distance to lunar diameter reads $a/(2R_{\odot}) = 108$. Dashed vertical straight lines mark the selected transition age, $(t_a - t^{\dagger})/\text{Gyr} = 0.57$ (left) and the assumed age of the Earth-Moon system (EMS), $(t_a - t_i)/\text{Gyr} = 4.57$ (right). The Roche limit, $a_R/R_{\oplus} = 2.898518$, is defined by a horizontal straight line. Values inferred from accurately studied paleontological data are plotted as diamonds, related to different authors when appropriate [25]. Source of data (from the left to the right): ER, BC (lower value preferred), WW (upper value preferred) [25]. See text (Introduction) for further details.

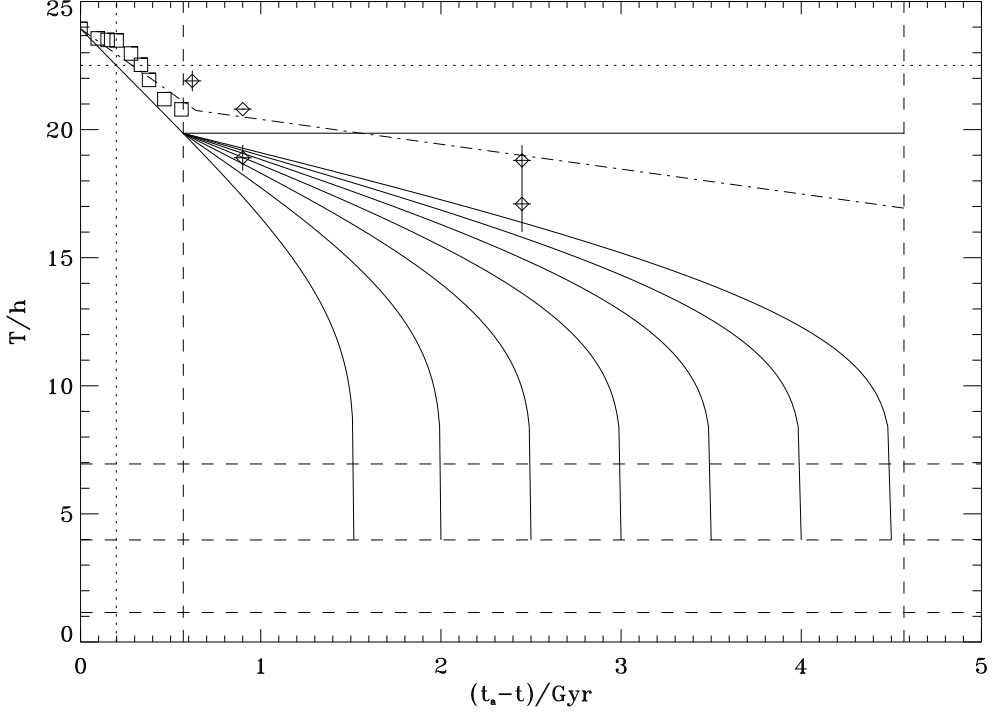


Figure 4: Predicted length of day (LOD) due to tidal friction, T/h , vs age (Gyr, back in time since J2000.0 date), $t_a - t$, for past 4.57 Gyr, according to Eq. (30), full lines, for different merging ages (from the left to the right), $(t_a - t^\ddagger)/\text{Gyr} = 1.516617, 2.0, 2.5, 3.0, 3.5, 4.0, 4.5, +\infty$ (no lunar recession). All features appearing in Fig. 2 are included within $0 \leq (t_a - t)/\text{Gyr} \leq 0.25$, but dotted straight lines define a special point, $(0.198499271, 22.50719109)$, on the dashed curve therein, for which the ratio of mean lunar distance to lunar diameter reads $a/(2R_\odot) = 108$. Dashed vertical straight lines mark the selected transition age, $(t_a - t^\dagger)/\text{Gyr} = 0.57$ (left) and the assumed age of the Earth-Moon system (EMS), $(t_a - t_i)/\text{Gyr} = 4.57$ (right). The Roche limit, $T_R/h = 6.948719$, the merging limit, $T^\ddagger/h = 3.982278$, and the Earth Poincaré limit, $T_P/h = 1.149728$, are defined by dashed horizontal straight lines. Dot-dashed lines are linear interpolations from paleontological data [16][3], extended back to $(t_a - t_i)/\text{Gyr} = 4.57$. A nonlinear trend also inferred from paleontological data [16][3] is shown as squares. Values inferred from accurately studied paleontological data are plotted as diamonds, related to different authors when appropriate [25]. Source of data (from the left to the right): ER, BC (lower value preferred), WW (upper value preferred) [25]. See text (Introduction) for further details.

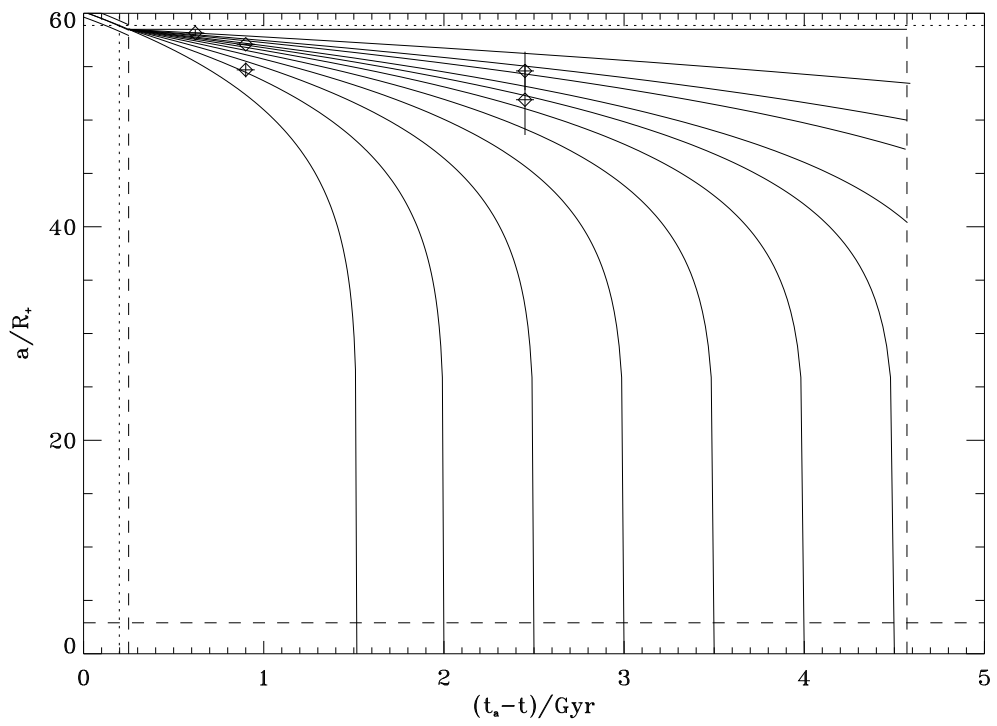


Figure 5: Same as in Fig. 3 but with regard to a later transition age, $(t_a - t^\dagger)/\text{Gyr} = 0.25$.

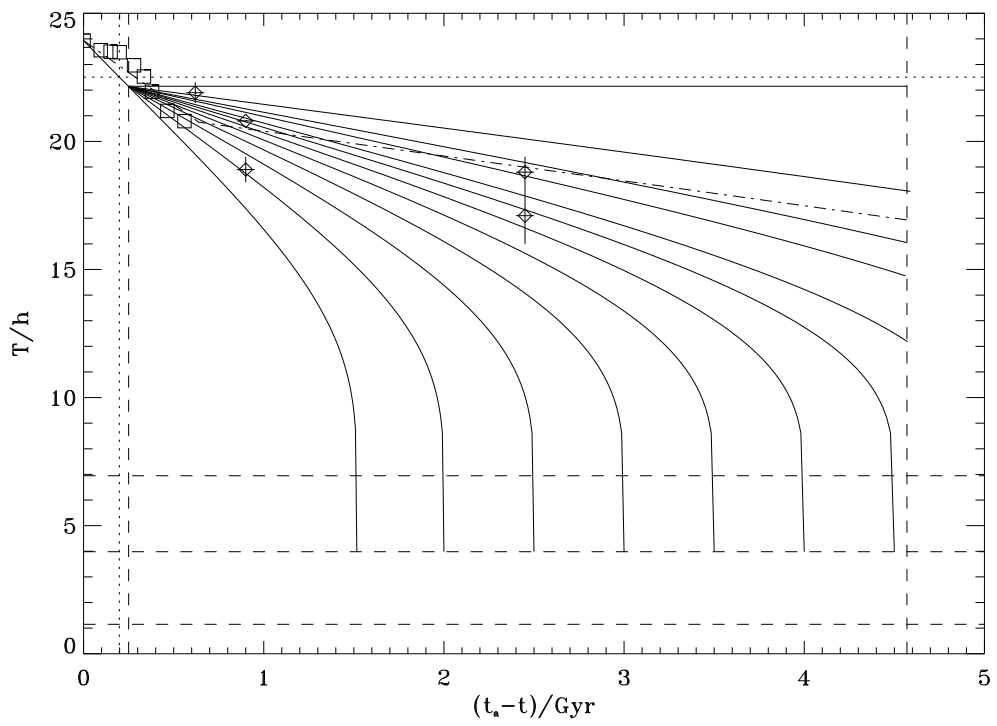


Figure 6: Same as in Fig. 4 but with regard to a later transition age, $(t_a - t^\dagger)/\text{Gyr} = 0.25$.

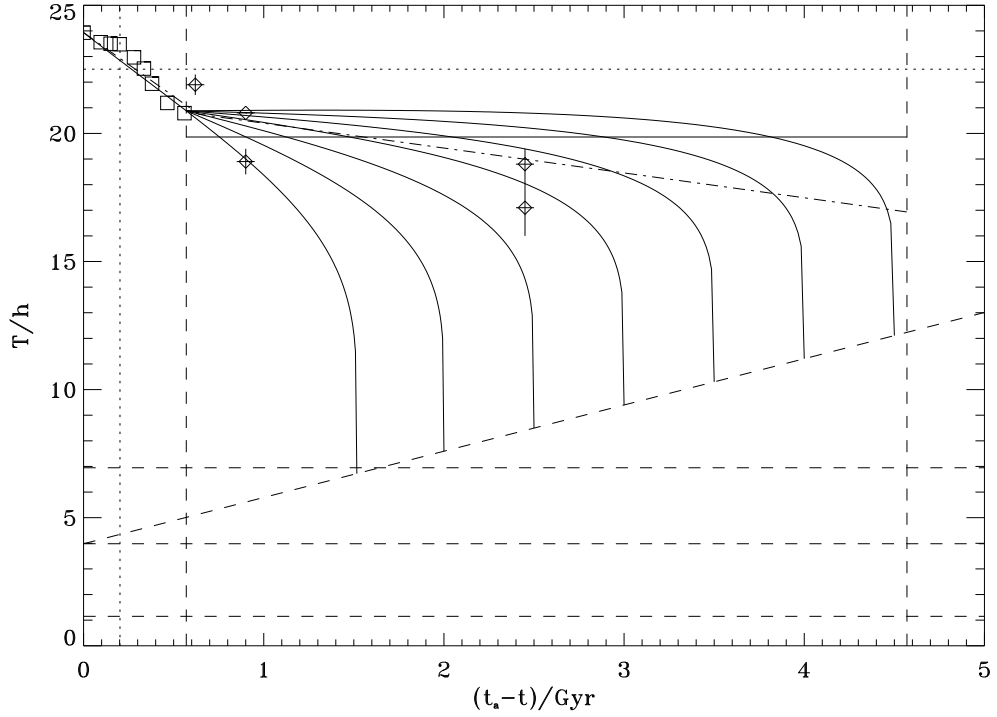


Figure 7: Same as in Fig. 4 but including, in addition to tidal friction, the effect of atmospheric tides and nontidal processes via an assumed time independent contribution yielding an additional term, $\Delta T/h = (65/36)(t_a - t)/\text{Gyr}$. The locus of merging configurations ($a = 0$) is shown as an inclined dashed straight line. See text for further details.

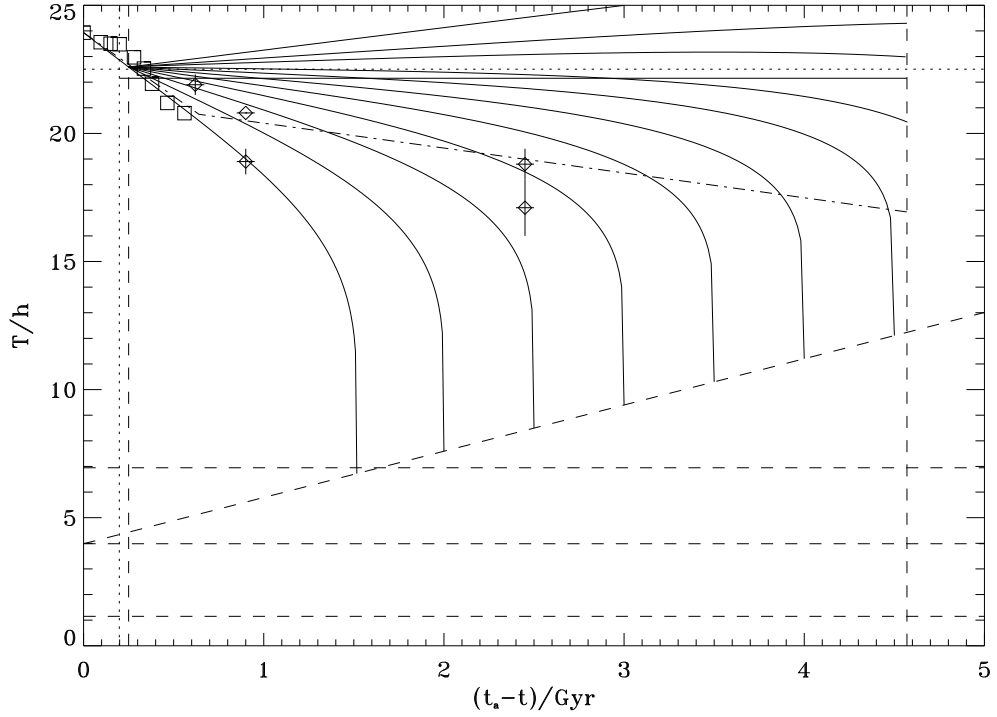


Figure 8: Same as in Fig. 6 but including, in addition to tidal friction, the effect of atmospheric tides and nontidal processes via an assumed time independent contribution yielding an additional term, $\Delta T/h = (65/36)(t_a - t)/\text{Gyr}$. The locus of merging configurations ($a = 0$) is shown as an inclined dashed straight line. See text for further details.